Proceedings World Geothermal Congress 2015
Melbourne, Australia, 19-25 April 2015

Reservoir Testing and Modeling of the Patua Geothermal Field, Nevada, USA

Sabodh K. GARG, Colin GORANSON, Stuart JOHNSON, John CASTEEL

Leidos Inc., 10260 Campus Point Dr., MS C2E, San Diego, CA 92121, USA

gargs@leidos.com

Keywords: Patua, Nevada, numerical modeling, natural state, pressure interference testing

ABSTRACT

To define the geothermal reservoir underlying the Gradient Resources Inc. (GRI) leases at the Patua Federal Geothermal Unit, GRI carried out an extensive exploration program consisting of geological, geochemical, and geophysical surveys, core hole drilling, well drilling, and pressure transient testing. Based on the data obtained from the well drilling and testing, a conceptual model of the Patua Geothermal Reservoir has been developed. The subsurface stratigraphy consists of a sequence of volcanic rocks overlying naturally-fractured granitic basement rocks. The geothermal reservoir is hosted by the naturally-fractured granitic rocks with high-permeability fractures striking along northeastern and orthogonal northwestern trends. Pressure interference data recorded by monitoring coreholes and shut-in wells during discharge testing support the concept of the lack of interconnection between coreholes completed in the volcanic rocks and production wells completed in the underlying granitic geothermal reservoir. Based on pressure interference data, the geothermal reservoir extends over at least ten (10) square miles.

The conceptual model formed the basis of a detailed 3-D numerical model of the geothermal field. The numerical model was developed using STAR, a general-purpose geothermal reservoir engineering simulator. Temperature and pressure profiles recorded in shut-in wells, and pressure interference data obtained during reservoir/well testing operations were used to condition the numerical model. The latter model is used to assess the capability of the reservoir to supply geothermal fluid for the Phase I 30 MWe (net) geothermal power plant.

1. INTRODUCTION

The Patua Hot Springs (Patua) geothermal prospect of Gradient Resources Inc., (GRI) is located approximately 38 miles east of Reno and about 10 miles east of the town of Fernley (Figure 1). Patua is located in the Basin and Range (i.e., the so-called Great Basin). In general, the Great Basin is characterized by abnormally high heat flow, hot springs, abundant extensional and normal faulting and high levels of microseismicity, as is Patua. In addition, five other currently operating geothermal power plants are located within 30 miles of the Patua prospect and two of them (i.e., Brady Hot Springs and Desert Peak) are about 10 miles northeast from Patua, attesting to the geothermal potential of the area.

Figure 1: Location of Patua geothermal field.

The stratigraphy in the Patua area consists of a variety of fine grained and diagenetically altered Quaternary sediments overlying a sequence of mafic-intermediate volcanic rocks interbedded with altered ash tuffs, which are underlain by a sequence of intermediate to silicic volcanics that have undergone pervasive argillic (clay) alteration. Core analysis and X-Ray diffraction completed on Tertiary volcanic rocks as well as Cretaceous granites, granodiorites, and tonalites indicates that argillic alteration of feldspathic minerals is the dominant alteration type at depths less than 7500 ft throughout the project area. The geothermal reservoir at Patua is hosted in fractured granitic rocks.

To assess the electric power potential of its leases at Patua, GRI undertook an extensive exploration program consisting of geological, geochemical, and geophysical surveys, core hole drilling, well drilling, and well discharge and pressure transient testing. Six coreholes (depths up to ~7,000 feet) as well as fifteen large-diameter production wells (depths up to ~12,000 feet) have been completed. Drilling targets for production wells have concentrated on intercepting faults noted in the seismic reflection data. Rock fragments (cuttings) and cores (side-wall and wire-line) from these zones show thermal alteration of the granitic complex.

Static pressure and temperature versus depth data have been obtained from all of the wells at Patua. Most of the coreholes at Patua are completed within the Tertiary volcanics, and exhibit conductive profiles. A conductive temperature versus depth profile is indicative of low permeability. The temperature data from large-diameter wells suggest the top of the geothermal reservoir to be located near the contact of the Tertiary volcanic section and granitic rocks at a depth of ~4,000 to 5,000 feet. Within the granitic

complex, the temperature profiles exhibit a much lower thermal gradient. In other words, only conductive temperature gradients have been recorded in the Tertiary volcanic rocks comprising the upper 5,000 feet of rocks in the Patua Unit and data showing permeable intervals with convective temperature profiles have been observed in select areas within granitic rocks at depths greater than 7,500 feet.

Since the middle of 2009, GRI has performed numerous pressure transient tests in order to characterize the permeability structure of the geothermal field. To-date, no tracer tests have been performed. Analysis of pressure transient data from numerous pressure transient tests performed at Patua indicates a rather wide range of transmissivities (50,000 to 150,000 md-ft). A preliminary distribution of transmissivity inferred from the various pressure transient tests is displayed in Figure 2; these transmissivity values were modified somewhat during the development of the 3-D numerical model of the Patua geothermal field in order to match the distribution of reservoir temperatures and pressures, and pressure transient data obtained during well testing.

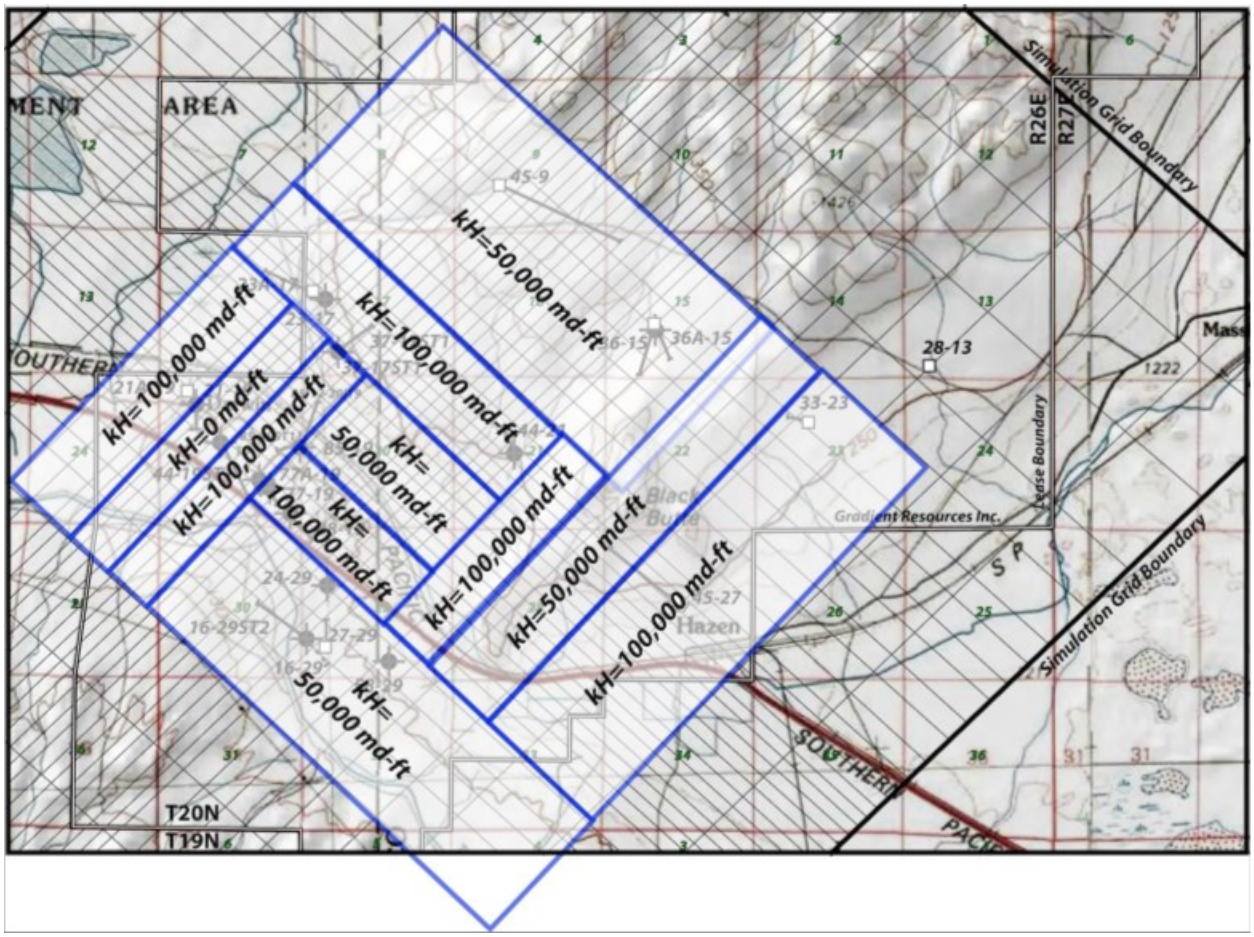

Figure 2: A preliminary distribution of reservoir transmissivity at Patua based on pressure transient tests.

This paper presents a 3-D numerical model of the Patua geothermal field. The quasi-steady natural state model was conditioned using static pressure and temperature surveys, and a field-wide pressure interference test performed in April 2012. Since large-scale production at Patua started only towards the end of 2013, little or no data are available at present (early 2014) for history-matching. The natural state model was used to investigate the response of the Patua reservoir for several production and injection scenarios capable of providing the required fluid supply for the Phase I 30 MWe (net) power plant for 20 years.

2. NUMERICAL MODEL

Temperature measurements in coreholes and deep wells in concert with results of pressure transient tests indicate that granitic rocks host the geothermal reservoir at Patua. The top of the granitic rocks generally is at about 5000 ft below ground surface (or about 1000 ft below sea level), and there is apparently, based on reservoir pressure testing, no pressure communication between the granitic geothermal reservoir system and the overlying volcanic rocks. It was, therefore, decided to place the top of the model grid at sea-level. The model grid extends 10,000 ft below sea-level. The bottom of the deepest well drilled to-date is located at about 6500 ft below sea-level; thus the model grid extends about 3500 ft below the bottom of the deepest well. In the current version of the numerical model, the bottom two layers (8000-10,000 ft bsl) are assumed to be impermeable.

To align with the major fault directions at Patua, the x- and y-directions of the model grid are oriented along NE and NW directions, respectively. The model grid covers an area of about 8.46x7.89 square miles in the horizontal (x-y) plane. With a reservoir thickness of 7000 ft, the transmissivity values shown in Figure 2 correspond to a horizontal permeability of either 7 md (kh = 50,000 md-ft) or 14 md (kh = 100,000 md-ft).

The model volume is divided in to a 36x35x10 grid in the x- and y- and z-directions respectively. In the z-direction, the grid blocks are of uniform thickness (1000 ft). In the x- and y-directions, grid blocks range from a low of 500 ft to a high of 3048 ft. The fine grid blocks (500 ft) are used to cover the region where the majority of the wells are located, and the coarsest resolution (3048 ft) is employed to model the region near to the model boundaries. Vertical Layers 5 through 7 (depths of ~7200 ft to 10,200 ft) are used as production and injection zones within the granitic reservoir system. An overlay of the grid over the Patua geothermal field is shown in Figure 3.

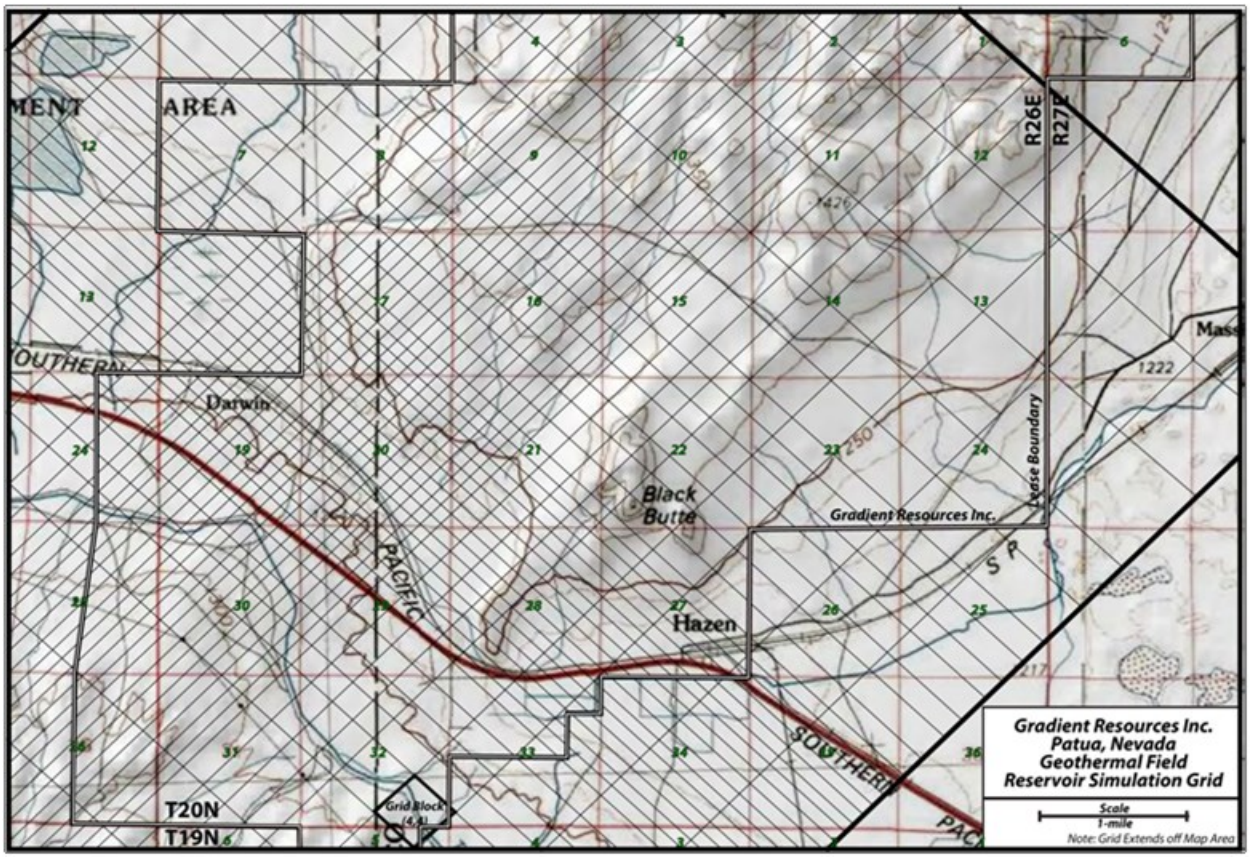

Figure 3: An overlay of the model grid over a map of the Patua geothermal field. The grid boundaries extend beyond the area shown in the figure. To provide a reference point, boundaries of grid block (4, 4) are indicated by dark color lines.

The 3-D numerical model was constructed using SAIC's STAR geothermal reservoir simulator (Pritchett, 2011). During the development of the natural-state model for the Patua geothermal field presented below, the boundary conditions were freely varied in order to match (1) the distribution of feedzone pressures (*i.e.,* pressure at the main fluid entry in a well), and (2) observed temperature profiles in wells. Numerous calculations were carried out; in the following, we will only describe the final case. Formation properties utilized for the Patua model are given in Table 1. Distribution of the formation properties within the model grid is shown in Figures 4 to 7. The vertical permeability at Patua appears to be rather low (*i.e.,* about 1 md in the reservoir area). None of the Patua wells exhibit a convective temperature profile (*i.e.,* a constant temperature with depth) nor is advection (lateral flow of thermal fluids) apparent in the well data, and a low vertical permeability is required for matching the temperatures versus depth recorded in Patua wells. The assumed horizontal permeabilities (and porosities) in layers k=3 to 9 are inferred from pressure transient data.

Both the top and the bottom boundaries of the grid are assumed to be impermeable. Unlike most of the hydrothermal fields developed to-date, it appears that Patua receives little or no mass recharge along the bottom boundary. Even the use of a small recharge results in some temperature reversals. In the final model presented in this paper only a conductive heat flux was assumed along the bottom boundary. The assumed distribution of heat flux is shown in Figure 8. The heat flux distribution was adjusted in order to match the observed temperatures in Patua wells. Along the top boundary (k=10), temperatures were prescribed. Where available, temperatures measured in Patua wells were used for this purpose. All vertical faces of the grid for layers k=3 to 10 are assumed to be permeable, and a constant pressure boundary is prescribed. Prescription of the pressure boundary is further described in the next section.

The reservoir fluid is a dilute NaCl brine, and can be represented for all practical purposes as pure water. All the calculations described here under were performed using pure water equation-of-state (WATSTM) embedded in the STAR geothermal reservoir simulator.

Table 1: Formation properties.

Formation Name	Intrinsic rock density (lbm/ft^3)	Rock grain specific heat ($Btu/lbm\ .^oF$)	Global Thermal Conductivity ($Btu/h.ft.^oF$)	Porosity	Permeability in x-direction (mdarcy)*	Permeability in y-direction (mdarcy)*	Permeability in z-direction (mdarcy)*
Volcanics	168.6	231.7	1.44	0.02	0.1	0.1	0.1
Granite#1	168.6	231.7	1.44	0.02	14	14	1
Granite#2	168.6	231.7	1.44	0.02	0.1	0.01	0.1
Granite#3	168.6	231.7	1.44	0.001	0.0001	0.0001	0.0001
Granite#4	168.6	231.7	1.44	0.02	7	7	1
Granite#5	168.6	231.7	1.44	0.02	2	7	1
Granite#1b	168.6	231.7	1.44	0.05	30	30	1
Granite#4b	168.6	231.7	1.44	0.05	30	30	1
Granite#1bb	168.6	231.7	1.44	0.06	14	14	1

*It is assumed here that 1 millidarcy is exactly equal to 10^{-15} m^2

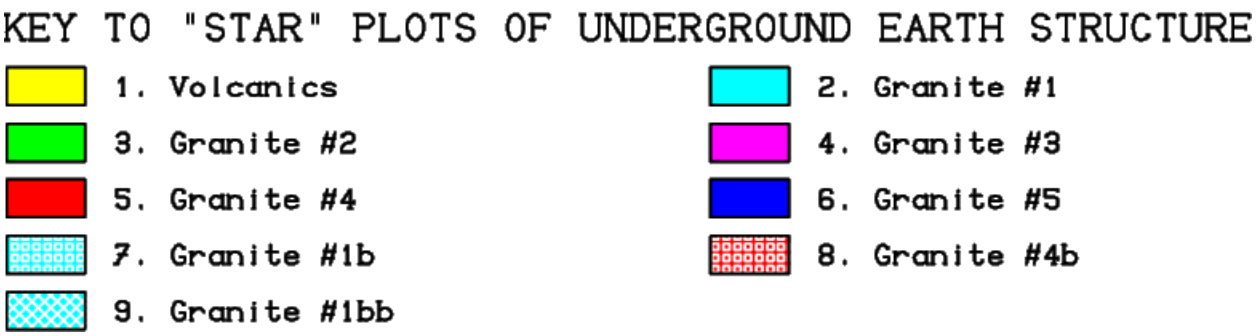

Figure 4: Color key to plots shown in Figures 5, 6, and 7.

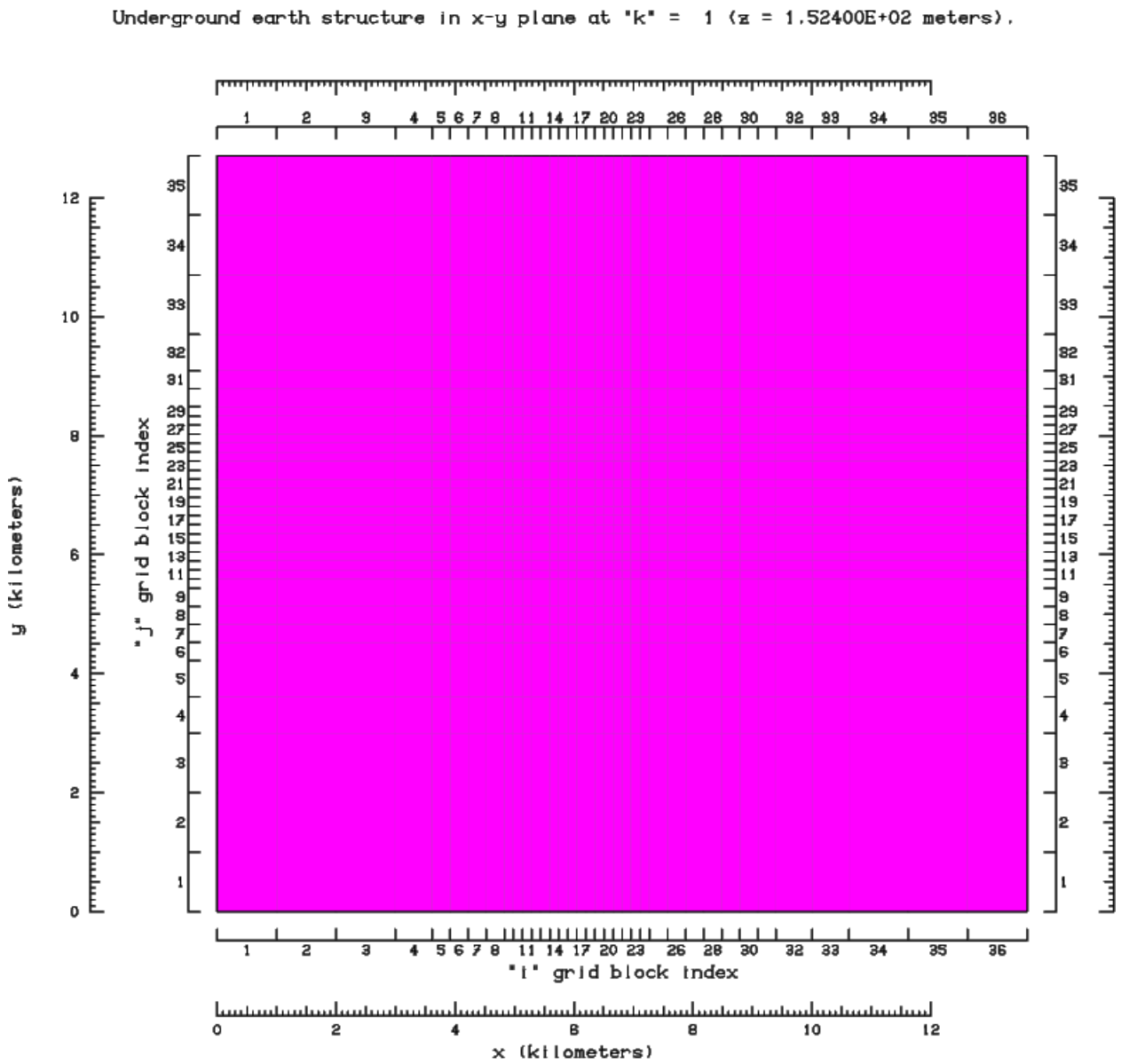

Figure 5: Formation distribution in layers k=1 and 2. Both of these layers are assumed to be impermeable, and are occupied by a single rock type (Granite #3).

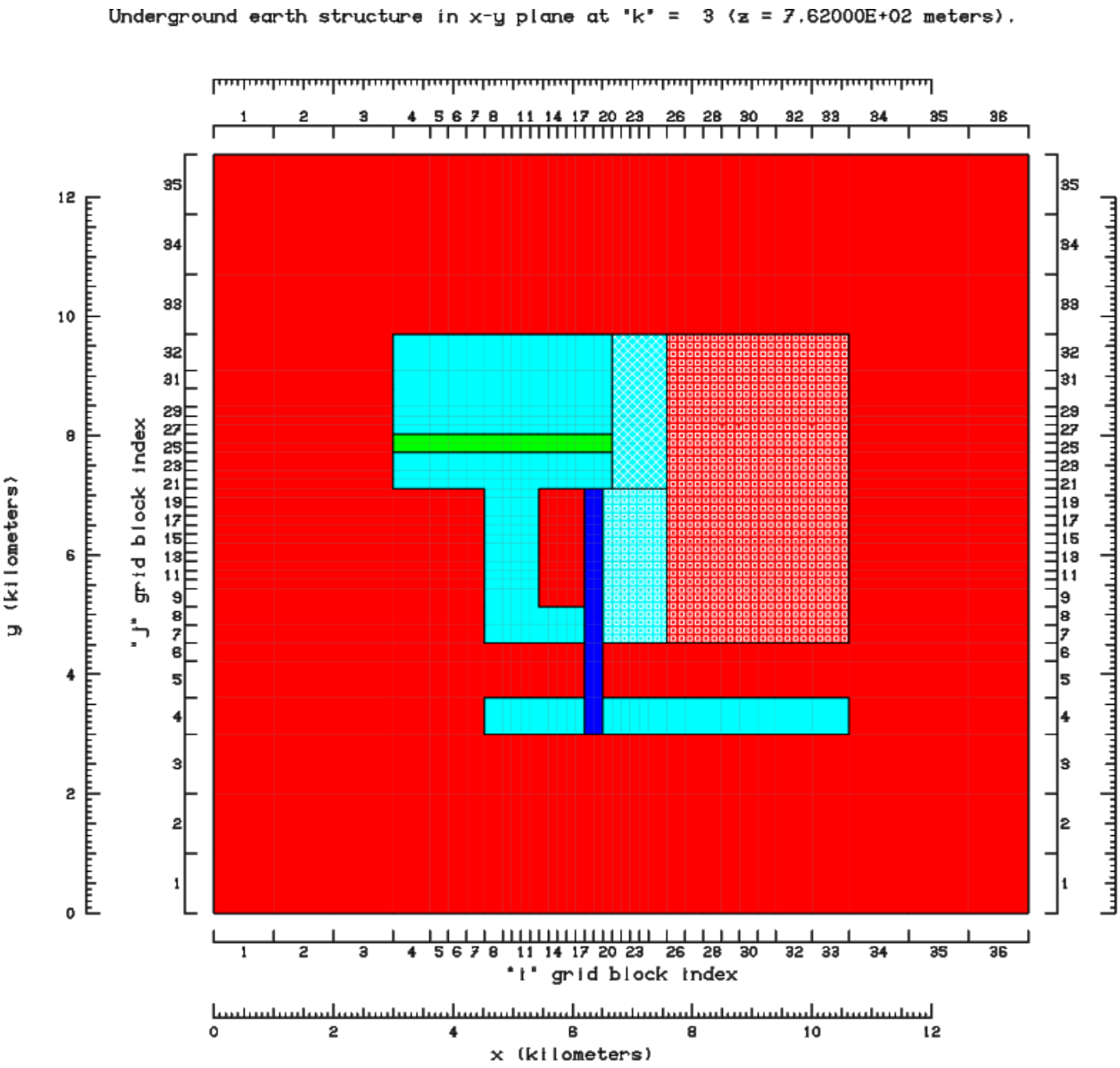

Figure 6: Formation distribution in layers k=3-9. The green rectangle (Granite #2) corresponds to the barrier that separates well 21-19 from well 77A-19. The blue rectangle (Granite #5) is the low permeability zone separating well 44-21 from section 19 and 29 wells.

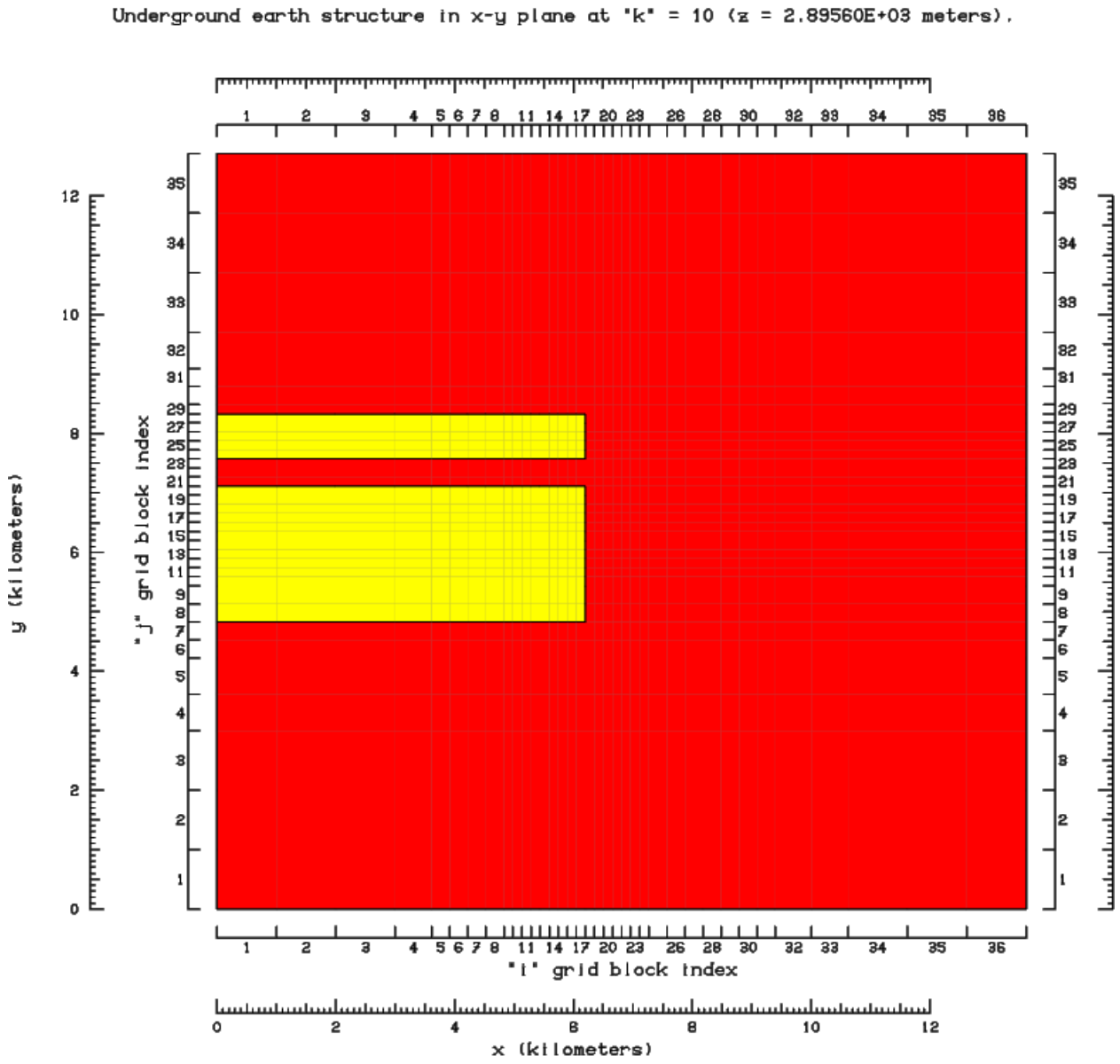

Figure 7: Formation Distribution in layer k=10. The red color corresponds to Granite #4. The volcanics are denoted by yellow color.

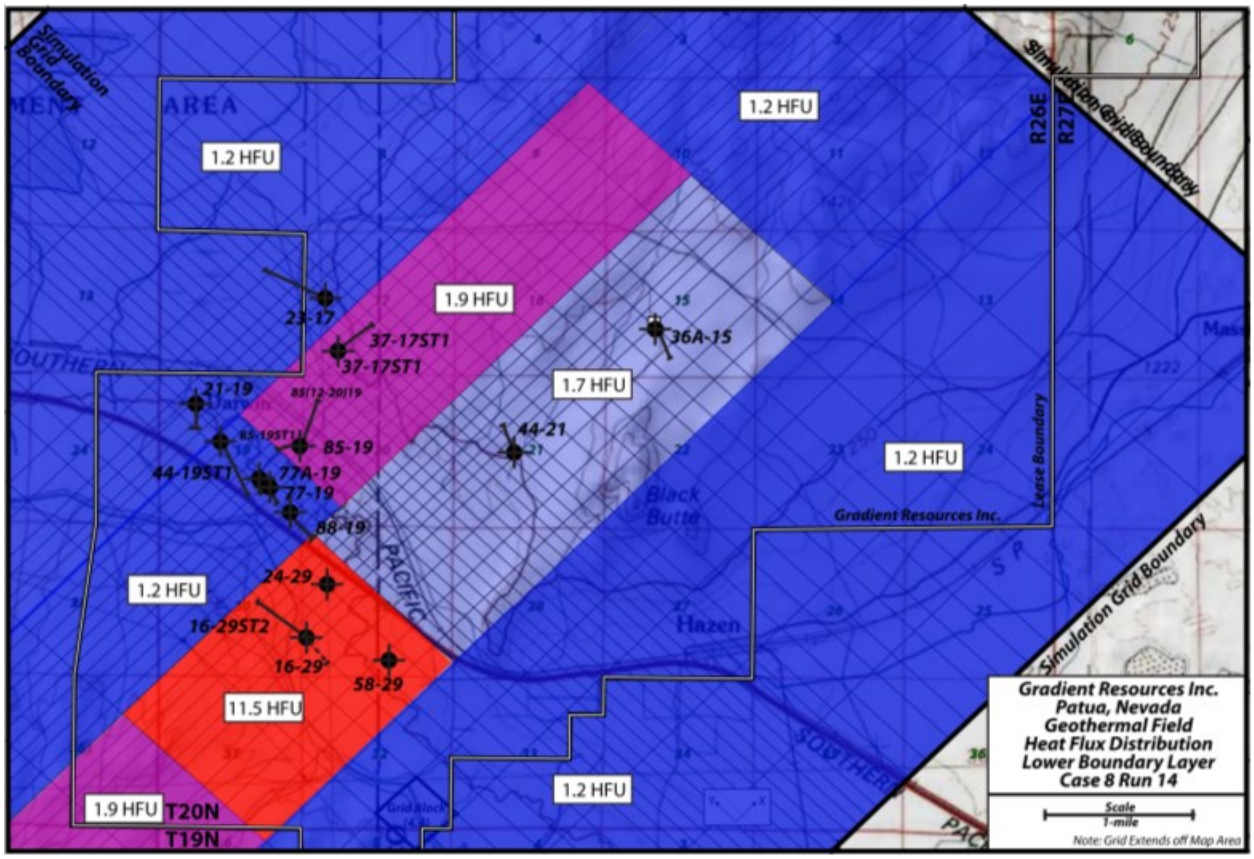

Figure 8: Heat flow (HFU) distribution along the bottom boundary.

3. COMPUTATION OF NATURAL STATE

The quasi-steady pre-production state (*i.e.,* natural state) was computed in two steps. In the first step, a constant pressure was imposed in grid blocks in layer k=9 along the boundary at x = 8.46 miles in order to initialize the pressures in the grid. All other vertical faces were assumed to be impermeable and thermally insulated. Starting from an essentially arbitrary cold state, the computation was marched forward in time for about 300,000 years. By the end of this step, pressures were found to be nearly steady with temperatures changing very slowly. In the second step, pressures computed for the grid blocks adjoining all the vertical faces of the grid in layers k=3-10 were imposed as constant pressure boundaries along these faces. All other boundary conditions were left unchanged. Within the grid, pressure and temperature distribution computed in step 1 were used as initial conditions. The calculation was run a further 300,000 years in order to obtain a quasi-steady natural state. By the end of the calculation, the thermal energy and mass content of the computational grid was changing extremely slowly; and the computed pressure and temperature distributions can be regarded as more or less steady over a time scale of 10 to 100 years.

The computed steady-state feedzone pressures are compared with measured values in Figure 9. Although the pressure data display some scatter, the fits to measured and computed values are in excellent agreement. Close agreement between measured and computed vertical pressures indicates that the vertical temperature distribution (and hence the pressure gradient) is correctly reproduced by the model.

The measured temperatures in two Patua wells are compared with calculated results from the model in Figures 10 and 11. Because of cross-flow between multiple fluid entries along a wellbore path (*i.e.*, circulation within the wellbore), the measured temperatures in wells do not necessarily reflect formation temperatures (*i.e.,* rock temperatures away from the wellbore). The measured temperature may equal the formation temperature only at the deepest (or shallowest) fluid entry in case of upflow (downflow) in the well. Our best estimates of feedzone temperatures based on flowing/static well pressure, temperature and spinner surveys are indicated by yellow symbols in Figures 10 and 11. An examination of these figures (as well as similar comparisons for other wells) shows that the computed values are generally in good agreement with data, especially at feedzone depths.

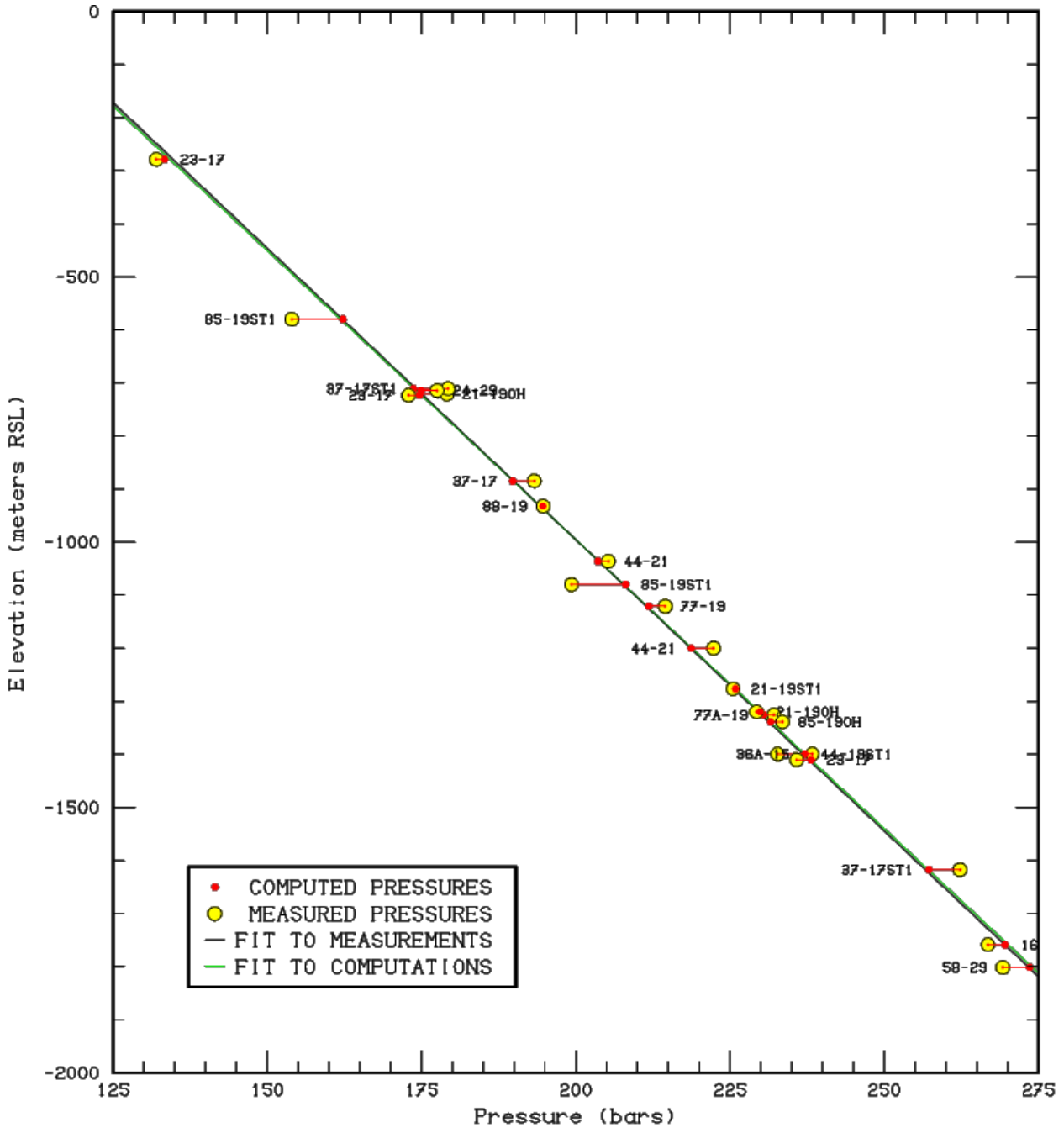

Figure 9: Comparison of computed feedzone pressures with measured values. Although the pressure data display some scatter, the fits to measured and computed values are in excellent agreement.

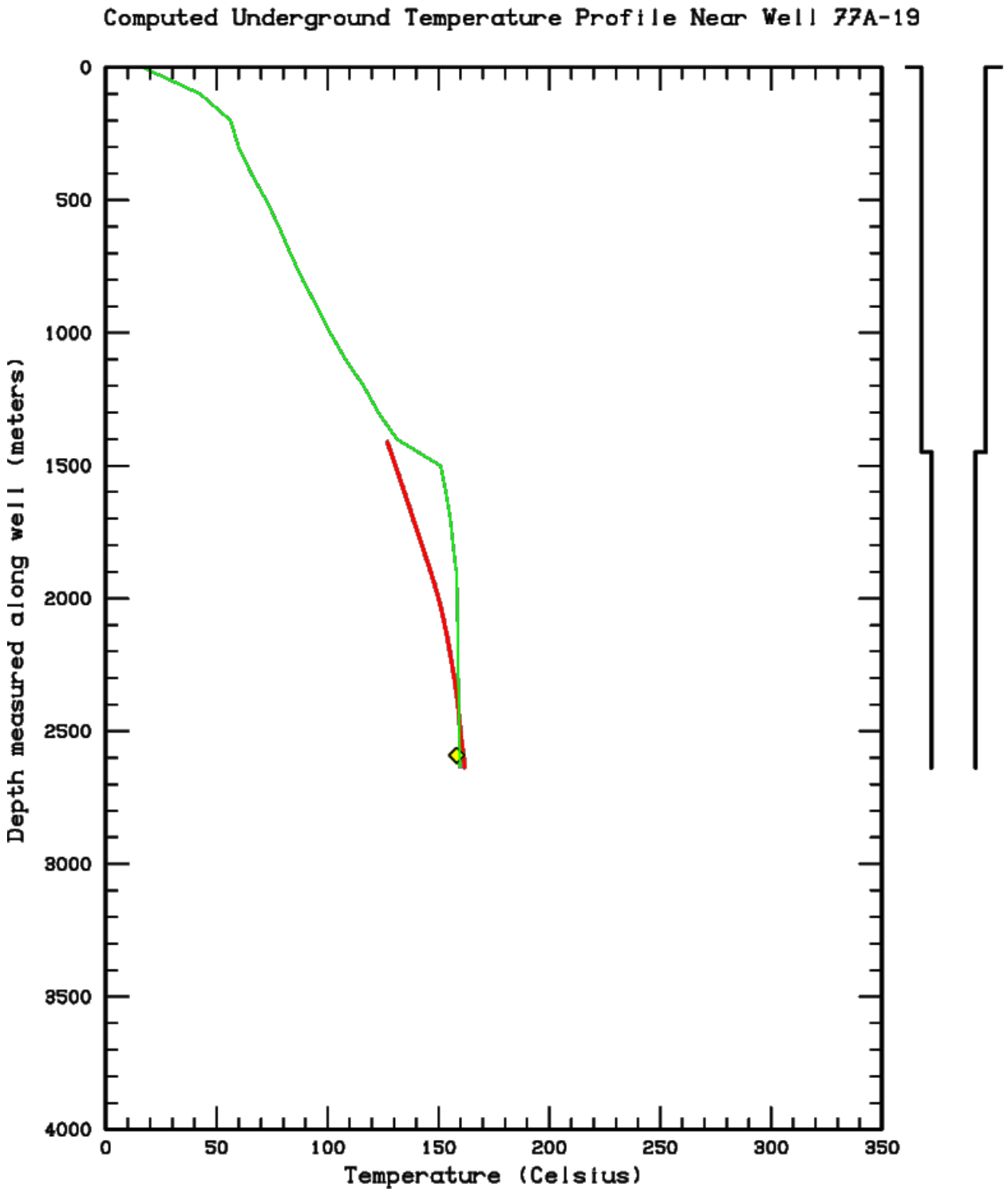

Figure 10: Comparison of measured temperature profile (green) with computed profile (red) for well 77A-19. The feedzone depth and estimated temperature are indicated by the yellow symbol.

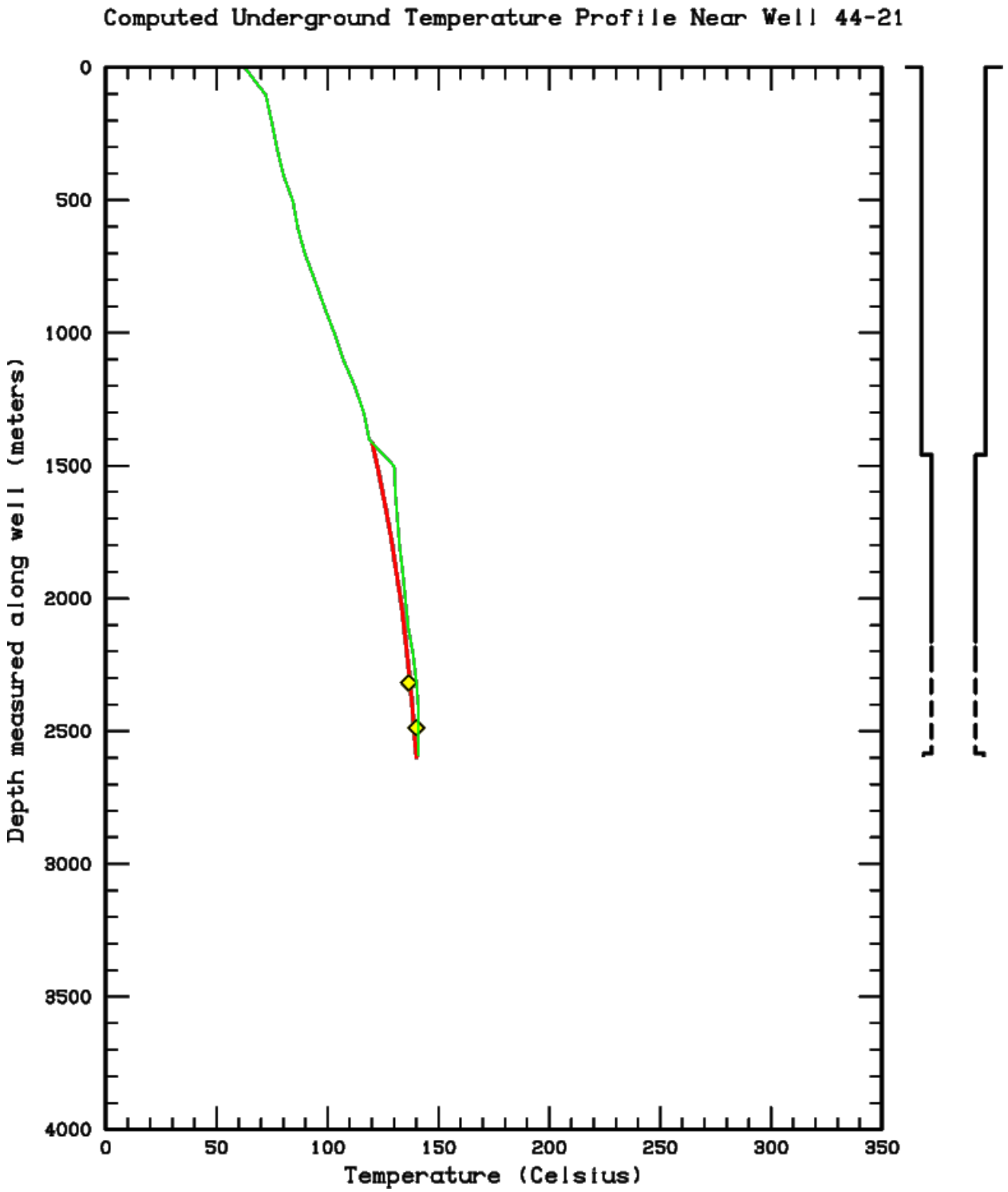

Figure 11: Comparison of measured temperature profile (green) with computed profile (red) for well 44-21. The feedzone depth and estimated temperature are indicated by the yellow symbol.

Reservoir models are best calibrated by matching historical production and injection data. At the present time (early 2014), long-term production and injection data are being gathered. In the following, pressure interference data recorded during a discharge and injection test of wells 44-21 and 37-17ST1 are utilized to calibrate the numerical model. A pump test of well 44-21 was performed from April 4, 2012 to April 12, 2012. A portion of the separated liquid was injected into well 37-17ST1. The discharge and injection histories were approximated using a few constant rate segments. The approximate histories are exhibited in Figures 12 and 13.

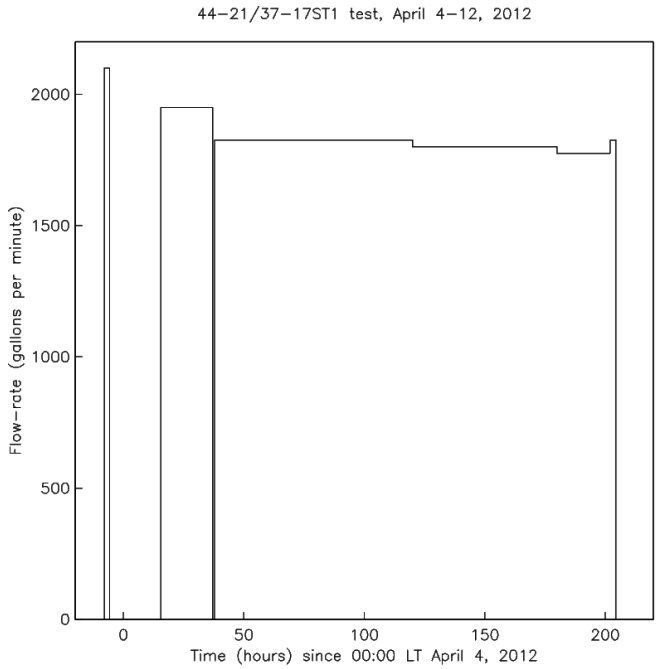

Figure 12: Averaged discharge rate history for well 44-21.

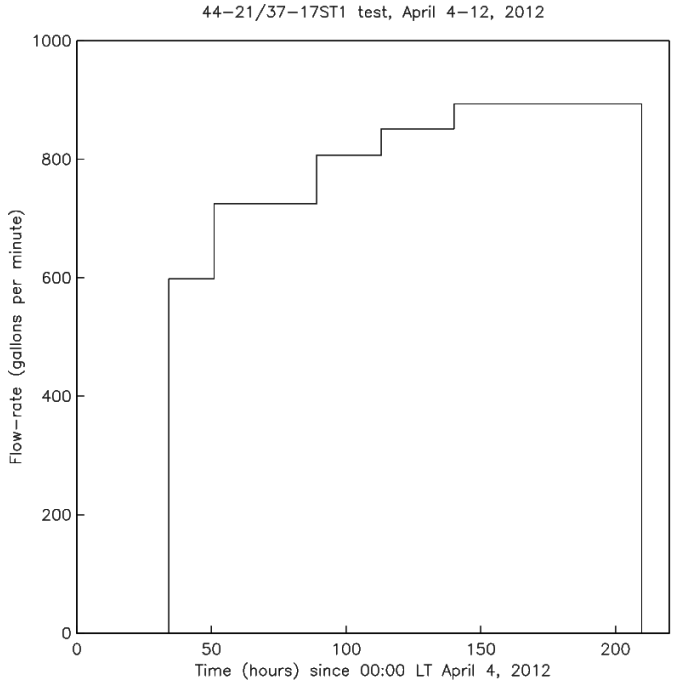

Figure 13: Averaged injection rate history for well 37-17ST1.

Prior to, during, and after the pump test of well 44-21, downhole pressures were monitored in nine (9) deep wells. No clear pressure interference response was detected in four of the wells. A pressure response was, however, observed in the remaining five wells. In order to simplify the model calculations, the pressure data were filtered to eliminate high frequency oscillations. The final natural state simulation model was used as the initial state for the pump test. Using a time step of 1 hour and the flow histories shown in Figures 12 and 13, the pressure response of the various observation wells was computed. A comparison between the observed pressure changes and the results of the numerical simulation is displayed for two of the observation wells in Figures 14 and 15. Considering the data quality, the agreement between the data and the simulated results is considered satisfactory. Thus, the simulation of the 44-21 pump test provides support for the natural state model described in the preceding sections.

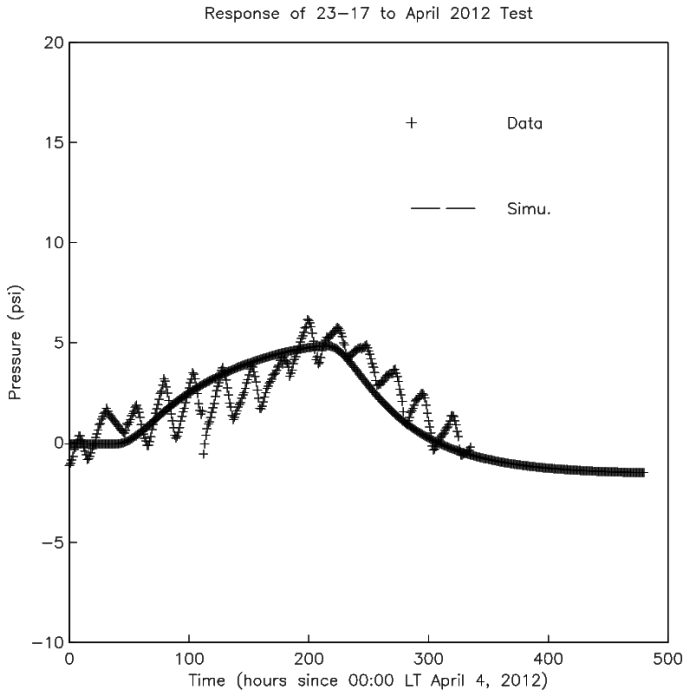

Figure 14: A comparison between measured and computed pressure response for well 23-17.

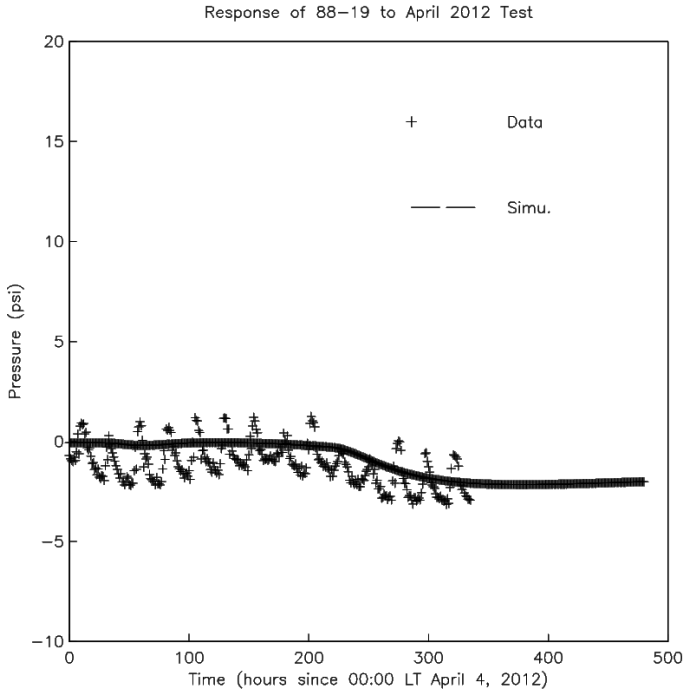

Figure 15: A comparison between measured and computed pressure response for well 88-19.

4. A PRODUCTION AND INJECTION SCENARIO

The Phase I 30 MWe (net) power plant at Patua was designed to operate with a supply of 16,000 gpm of hot water at a temperature of 315 ^{o}F. All of the produced fluid will be injected back in to the reservoir at a temperature of ~150 ^{o}F. The natural state model was used to forecast the response of the Patua reservoir for several future production and injection scenarios capable of providing the required fluid supply for 20 years. In the following, we describe Case 8; this scenario assumes that 7 multi-legged production and 6 multi-legged injection wells will be used. The well layout for this case is illustrated in Figure 16. At the time (fall of 2012) this scenario was run, several of the boreholes had yet to be drilled and tested.

For purposes of simulation presented below, each multi-legged well is represented by a single equivalent well at the average location of individual well-leg feed zones with the composite productivity (or injectivity) index. The grid blocks used in the numerical model are much larger than the typical well diameter. Consequently, it is necessary to use a sub-grid model in order to compute well pressures. In the following, it is assumed that all the wells are open to the formation in the depth interval from 3000

to 6000 ft below sea-level (*i.e.*, vertical grid blocks 5, 6, and 7); the datum level for well pressure calculations is taken to be at the center of layer 7 (*i.e.,* 3500 ft below sea-level). The sub-grid formulations of Pritchett and Garg (1980) and Peaceman (1983) were used to represent the wells in the simulation.

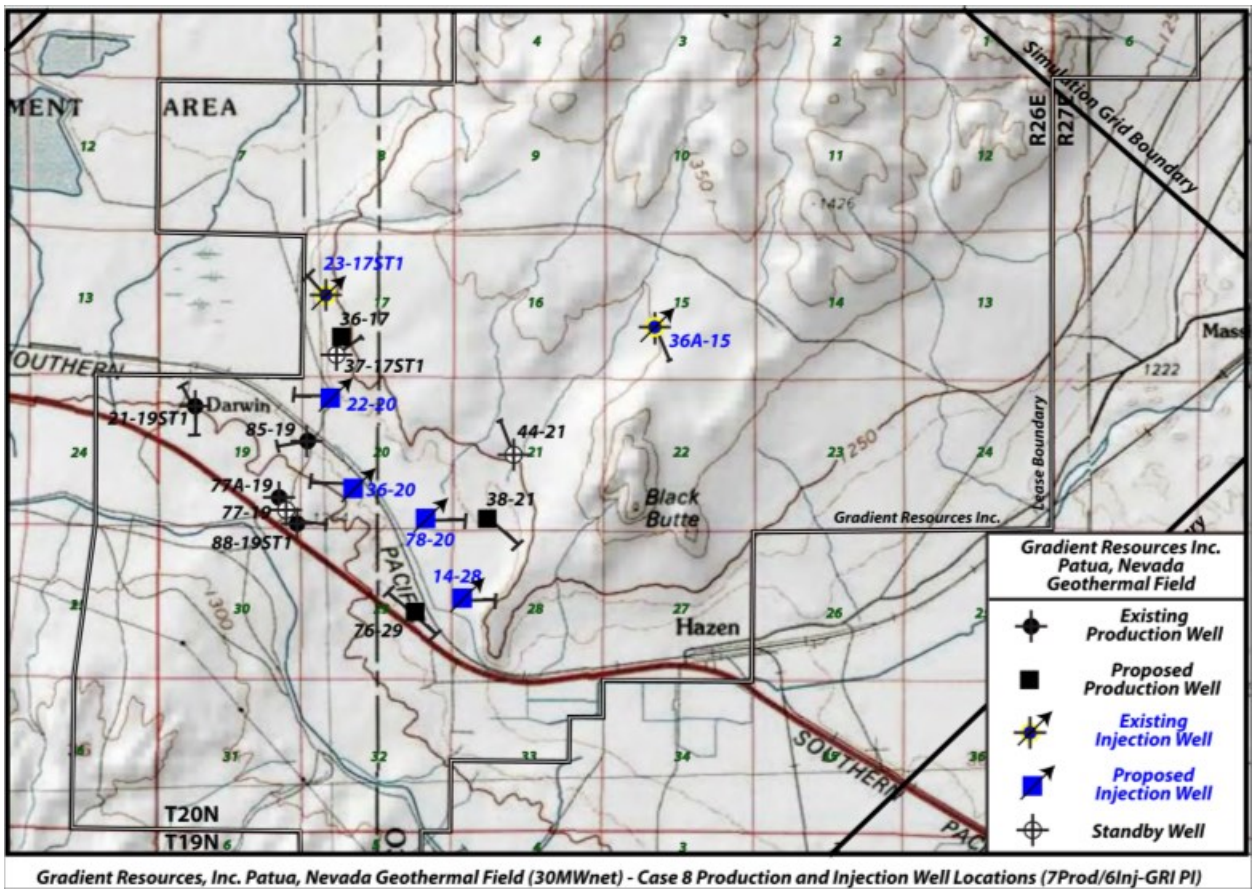

Figure 16: Production and Injection well locations.

The total discharge (or injection) rate from the Patua geothermal field is assumed to be constant at 960 kg/s (7.62 million lbm/hour) for the entire 20-year period. The latter mass rate corresponds to 16718 gpm at 315 ^{o}F and 15523 gpm at 150 ^{o}F. The total discharge (or injection) rate was divided among the various production (or injection) wells so as to obtain approximately the same datum level pressure at 20 years. The computed datum level pressures for the seven production wells are displayed in Figure 17. Most of the pressure decline in production wells occurs during the first few months; thereafter, the pressure changes are minimal. In contrast to the production wells, pressure changes in the injection wells (Figure 18) are more gradual. The pressure changes in injection wells after the first few months are mainly due to the cooling of the reservoir volume around the injection wells. The average enthalpy history of the produced fluid is shown in Figure 19. The changes in average enthalpy are quite small. For the entire 20-year production period, the average temperature of the produced fluids varies by about 7 ^{o}F.

To numerically investigate the possible effect of cold fluid injection on the discharge enthalpy (and temperature), a separate tracer was injected in to each of the six injection wells. In addition, a tracer was introduced to monitor the fluid influx from the vertical grid boundaries. Tracer returns were monitored in all of the seven production wells. Computed results show that none of the mass influx from the constant pressure vertical boundaries makes it to the production wells. Also, very little of the fluid injected into well 36A-15 appears in any of the seven production wells; the injected fluid, however, remains in the reservoir and thus provides pressure support. Three of the production wells do not exhibit any significant cooling effects; other wells undergo a temperature decline ranging from 8 ^{o}F to 30 ^{o}F.

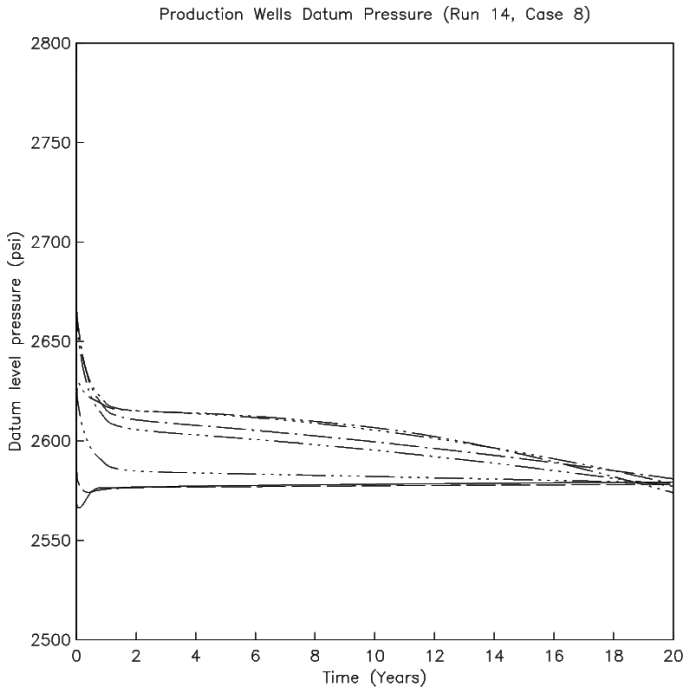

Figure 17: Computed datum level pressures in Patua production wells from t =0 to t=20 years.

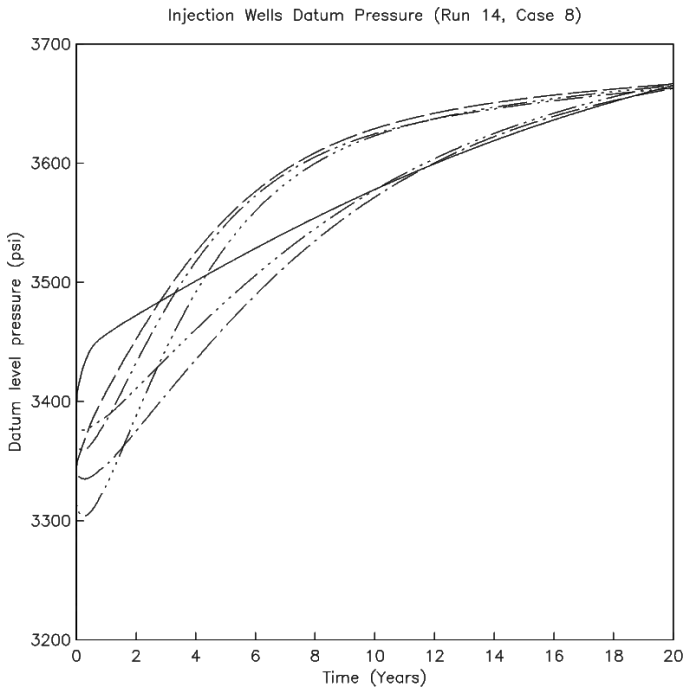

Figure 18: Datum level pressure changes in Patua injection wells from t=0 to t=20 years.

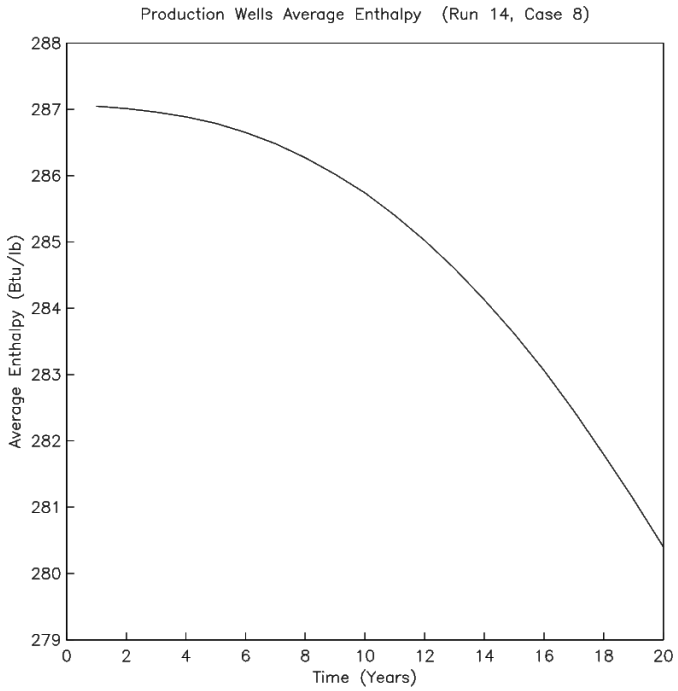

Figure 19: Average downhole enthalpy history of the produced fluid at Patua.

5. CONCLUDING REMARKS

The natural state numerical model presented above correctly reproduces the presently available data for feedzone temperatures and pressures, and pressure interference test results. The numerical model was used to investigate the feasibility of producing sufficient fluid to supply the Phase I 30 MWe (net) power plant at Patua. Commercial production and injection operations started at Patua in the fall of 2013. Availability of large scale production data over the next year or two will make it possible to further assess the numerical model, and to refine it as needed to reflect the enhanced knowledge obtained for the Patua geothermal field. The refined natural state model can then be used to examine additional production and injection scenarios.

REFERENCES

Peaceman, D.W.: Interpretation of well-block pressures in numerical reservoir simulation with nonsquare grid blocks and anisotropic permeability, *Society of Petroleum Engineers Journal,* **23(3),** (1983), 531-543.

Pritchett, J.W.: STAR User's Manual Version 11.0, Science Applications International Corporation, San Diego, CA, U.S.A. (2011).

Pritchett, J.W. and Garg, S.K.: Determination of effective wellbore radii for numerical reservoir simulations, *Water Resources Research,* **16(4)**, (1980), 665-674.